IL NUOVO CIMENTO VOL. 10 B, N. 2 11 Agosto 1972

Orbital and Vortical Motion in the Kerr Metric.

F. DE FELICE and M. CALVANI

Gruppo di Astrofisica Teorica - Padova
Istituto di Fisica «Galileo Galilei» dell'Università - Padova
Istituto di Astronomia dell'Università - Padova

(ricevuto il 20 Dicembre 1971)

Summary. — The motion is analysed, in general, in the Kerr metric with the use of first integrals. Some of the high-energy particles and photons are found to move in a giant vortex around the axis of symmetry above and below the equatorial plane, dragged by the gravitational field.

1. – Introduction.

Because of the increasing importance of rotation in relativistic configurations (spinors, gravitational collapse, etc.) several authors have looked for the effects of gravity on light rays emitted by rotating bodies ([1,2]).

The aim of the present paper is to investigate in detail the laws of motion in the Kerr metric, outside the equatorial plane as well as off the axis of symmetry. These last two cases have been investigated respectively by ([1-4]) and ([5]), while the general motion has been outlined by CARTER ([6]).

([1]) R. H. BOYER and R. W. LINDQUIST: *Journ. Math. Phys.*, **8**, 265 (1967).
([2]) R. H. BOYER and T. G. PRICE: *Proc. Cambridge Phil. Soc.*, **61**, 531 (1965).
([3]) F. DE FELICE: *Nuovo Cimento*, **57** B, 351 (1968).
([4]) F. DE FELICE: *Mem. Soc. Astr. Ital.* (to appear).
([5]) B. CARTER: *Phys. Rev.*, **141**, 1242 (1966).
([6]) B. CARTER: *Phys. Rev.*, **174**, 1559 (1968).

2. – The general ϑ-motion.

The Kerr metric describes stationary axisymmetric gravitational fields in vacuum ([7]). It is characterized by two parameters a and m, which are associated with the specific angular momentum and active gravitational mass of the source in geometrical units ([1,8]).

We shall confine ourselves to the case $a = m$ because of the important role it has had in recent investigations ([9,10]).

The Kerr metric reads in this case

$$(1)\qquad \mathrm{d}s^2 = \mathrm{d}r^2 + 2a\sin^2\vartheta\,\mathrm{d}r\mathrm{d}\vartheta + (r^2+a^2)\sin^2\vartheta\,\mathrm{d}\varphi^2 + \\ + (r^2 + a^2\cos^2\vartheta)\,\mathrm{d}\vartheta^2 - \mathrm{d}t^2 + \frac{2ar}{r^2+a^2\cos^2\vartheta}(\mathrm{d}r + a\sin^2\vartheta\,\mathrm{d}\varphi + \mathrm{d}t)^2,$$

where use is made of the $(r, \vartheta, \varphi, t)$ co-ordinates in the Boyer-Lindquist form ([1]).

The equations of motion are given by a suitable analysis of the Hamilton-Jacobi equation associated with (1) ([5]), leading to the following first integrals:

$$(2)\qquad \left(-1 + \frac{2ar}{\Sigma}\right)\dot{t} + \frac{2ar}{\Sigma}(a\sin^2\vartheta\,\dot{\varphi} + \dot{r}) = -\gamma,$$

$$(3)\qquad \frac{2a^2r\sin^2\vartheta}{\Sigma}\dot{t} + a\sin^2\vartheta\left(1 + \frac{2ar}{\Sigma}\right)\dot{r} + \left[(r^2+a^2)\sin^2\vartheta + \frac{2a^3r}{\Sigma}\sin^4\vartheta\right]\dot{\varphi} = l,$$

$$(4)\qquad \Sigma^2\dot{\vartheta}^2 = L^2 - a^2\cos^2\vartheta(\varepsilon - \gamma^2) - \frac{l^2}{\sin^2\vartheta},$$

$$(5)\qquad \Sigma^2\dot{r}^2 = (al + 2ar\gamma)^2 + \delta\left[-\varepsilon\Sigma + (\Sigma + 2ar)\,\dot{\gamma}^2 - \Sigma^2\dot{\vartheta}^2 - \frac{l^2}{\sin^2\vartheta}\right],$$

with

$$\Sigma = r^2 + a^2\cos^2\vartheta,$$

$$\delta = (r-a)^2.$$

In (2)-(5), γ is the total energy of the particles; L and l are constants of motion which are easily interpreted as the total angular momentum and its φ-component, in the limit $a = 0$. ε is a sign indicator which is $+1$ or zero according to whether the geodesic is timelike or null.

([7]) R. P. KERR: *Phys. Rev. Lett.*, **11**, 522 (1963).
([8]) J. LENSE and H. THIRRING: *Phys. Zeit.*, **19**, 156 (1918).
([9]) J. BARDEEN: *Nature*, **226**, 64 (1970).
([10]) J. M. BARDEEN and R. V. WAGONER: *Astrophys. Journ.*, **167**, 359 (1971).

On any curve, the domain of the allowed values of the co-ordinates is given, as is well known, by the equations of motion and by the initial conditions. In ref. [3] one of us has looked for the domain of the allowed values of the radial co-ordinate r on the equatorial geodesic in the Kerr metric.

Here we shall extend that method of analysis to investigate, in general, the behaviour of the angular co-ordinate ϑ in the geodesic motion. Putting $\varepsilon = +1$ in (4), we can learn how massive particles move. We have

$$L^2 + a^2 \Gamma \cos^2 \vartheta - \frac{l^2}{\sin^2 \vartheta} = 0 , \tag{6}$$

where

$$\Gamma = \gamma^2 - 1 .$$

We solve eq. (6) with respect to l^2 and draw the surface $l^2 = l^2(L^2, \vartheta, \Gamma)$.

Consider $\Gamma > 0$; the surface l^2 is zero at $\vartheta = 0$ and $\vartheta = \pi$. Its first ϑ-derivative

$$l^2_{,\vartheta} = \sin 2\vartheta [L^2 + a^2 \Gamma \cos 2\vartheta] \tag{7}$$

is zero at $\vartheta = 0$, $\vartheta = \pi/2$, $\vartheta = \pi$ and along the curve

$$L^2 = -\Gamma a^2 \cos 2\vartheta . \tag{8}$$

The shape of (8) is the curve a) in Fig. 1. The shapes of l^2 are given in Fig. 2

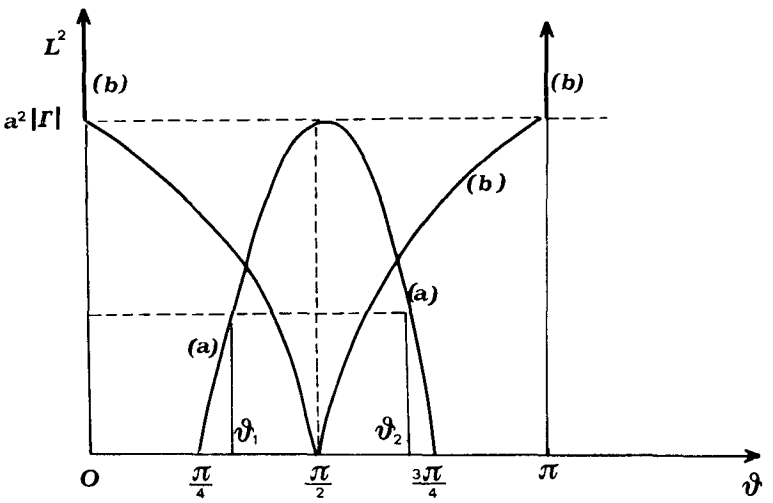

Fig. 1. – The analytic behaviour of eq. (8) (curve a)) and that of eq. (10) (curve b)) are given on the (L^2-ϑ)-plane.

for $L^2 < a^2\Gamma$ and for $L^2 > a^2\Gamma$. In Fig. 2, when $L^2 < a^2\Gamma$, the maximum for l^2 occurs at

$$l^2_{\max} = \frac{1}{4a^2\Gamma}(L^2 + a^2\Gamma)^2$$

and the minimum at $l^2 = L^2$; when $L^2 > a^2\Gamma$, l^2 has a maximum at $l^2 = L^2$ only.

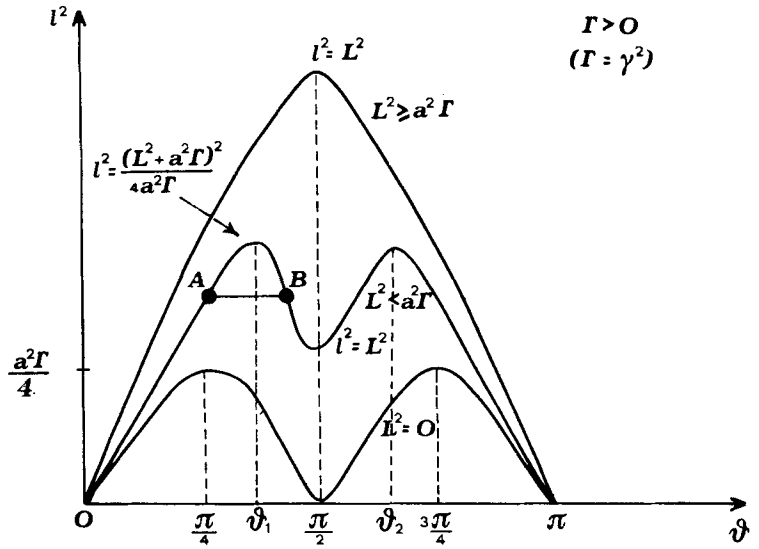

Fig. 2. – Sections with $L^2 = \text{const}$ of the surface $l^2_+ = l^2_+(L^2, \vartheta, \Gamma)$ given by eq. (6) with $\Gamma > 0$ or $\Gamma = \gamma^2$.

When $\Gamma = 0$ we notice from (6) that, with our choice of the co-ordinate system, the rotation does not affect the ϑ-motion on the geodesics. The particles with $\Gamma = 0$, however, do not move as in the Schwarzschild field ($a = 0$) because their φ-motion is now different, as is easy to deduce from (2)-(5).

Consider now the case $\Gamma < 0$. Equation (6) may be written again as

$$l^2 = \sin^2\vartheta[L^2 - a^2|\Gamma|\cos^2\vartheta]. \tag{9}$$

The zeros for l^2 are at $\vartheta = 0$, $\vartheta = \pi$ and along

$$L^2 = a^2|\Gamma|\cos^2\vartheta\,. \tag{10}$$

The locus where l^2 is zero in (9) is the curve b) in Fig. 1. It is easy to see that in the region of definition for l^2 there are no other zeros of its first derivative except $\vartheta = \pi/2$, where l^2 has a maximum equal to L^2. The general shape of

the surface $l^2 = l^2(L^2, |\Gamma|, \vartheta)$ is given in Fig. 3. The maximum occurs at $l^2 = L^2$.

Let us now put in (4) $\varepsilon = 0$, to describe the behaviour of photons. Equation (4) is the same as for $\varepsilon = +1$, provided we put $\Gamma = \gamma^2$. The relative

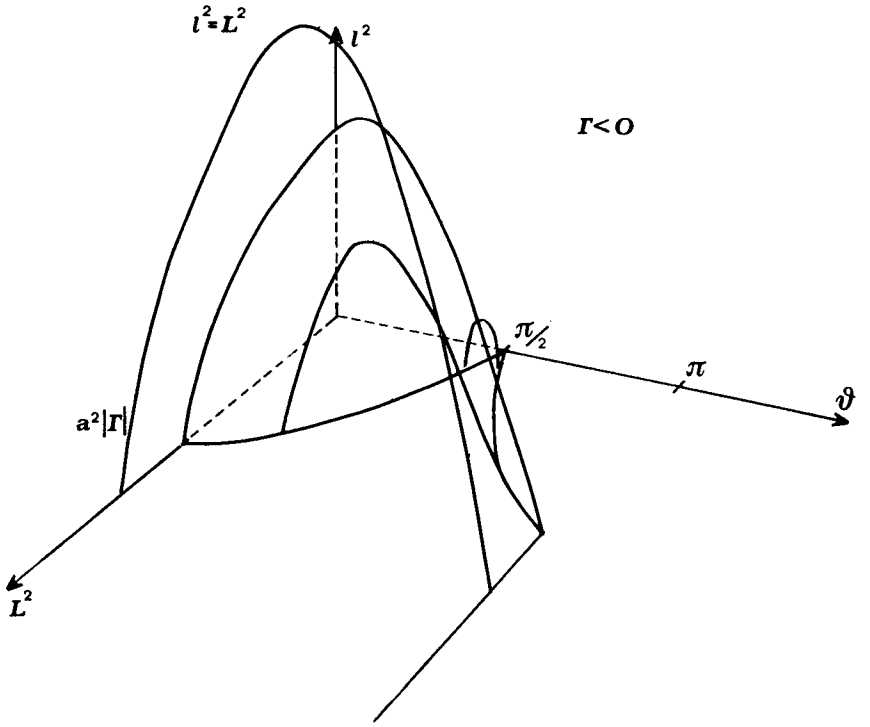

Fig. 3. – A three-dimensional picture of the surface $l_-^2 = l_-^2(L^2, \vartheta, \Gamma)$ given by eq. (9) with $\Gamma < 0$.

loci of zeros for ϑ are again given by Fig. 2. The reality requirement for l^2 confines the motion inside the surfaces (6) and (9). We are now in a position to draw attention to a peculiar relativistic effect. In Fig. 2 it is evident that for (*)

$$\text{(11)} \qquad \begin{cases} L^2 < a^2\Gamma, \\ \dfrac{1}{4a^2\Gamma}(L^2 + a^2\Gamma)^2 \geqslant l^2 > L^2, \end{cases}$$

the motion is confined to the space between two coaxial hyperboloids with angles ϑ_A and ϑ_B (Fig. 2), and never reaches the equatorial plane [5]. There is

(*) The same inequalities holding for photons with $\Gamma = \gamma^2$. In the following we shall speak about particles without specifying their nature.

no stable motion at $\vartheta = \text{const} = \pi/2$, while we can have two stable modes at $\vartheta = \text{const}$ when

$$l^2 = \frac{(L^2 + a^2\Gamma)^2}{4a^2\Gamma}.$$

In this case the motion occurs on the surfaces of the hyperboloids with semi-angles

$$\vartheta_{\pm}^{-} = \frac{\pi}{2} \pm \frac{1}{2}\cos^{-1}\frac{L^2}{a^2\Gamma}. \tag{12}$$

The angles $\vartheta_{\pm}$ range from $\pi/4$ at $L^2 = 0$ to $\pi/2$ at $L^2 = a^2\Gamma$ (Fig. 1, curve *a*)).

Particles and photons with parameters l and L in the range (11) are confined by the gravitational field to the northern or the southern hemisphere of the rotating body.

We can summarize the previous results, recalling the following facts. The motion in the equatorial plane ($\vartheta = \pi/2$) occurs when $L = l$. It is stable for all ($\Gamma \leqslant 0$)-particles and for the ($\Gamma > 0$)-particles (or photons with $L^2 \geqslant a^2\Gamma$; it is unstable for the latter when $L^2 < a^2\Gamma$. In this case, stable motion with $\vartheta = \text{const}$ is allowed with

$$l^2 = \frac{(L^2 + a^2\Gamma)^2}{4a^2\Gamma} \qquad (\Gamma = \gamma^2 \text{ for photons}).$$

Along the axis ($\vartheta = \text{const} = 0$), it seems that no stable motion is allowed, owing to the dragging along by the gravitational field. The particles are then forced to spiral around it in a sort of a giant vortex. The optical distortion produced by the vortical motion of photons may be relevant to astronomical observations, but more information may be achieved once the behaviour of $\dot{\varphi}$ is understood as it is for the equatorial plane [4]. Work in this sense is now in progress (*).

3. – The radiation emission. The r-motion for photons.

Let us now investigate the photon emission. Introduce for simplicity the following nondimensional quantities:

$$\lambda = \frac{l}{2a}, \quad \mathscr{L} = \frac{L}{2a}, \quad \varrho = \frac{r}{2a}, \tag{13}$$

and put $\gamma = 1$.

(*) When $\Gamma = 0$, stable motion with $\vartheta = \text{const}$ occurs when $l = L = 0$. In this case, however, the equations of motion (2)-(5) indicate that the particles also move on the surface of hyperboloids with semi-angles ranging from $\pi/2$ to zero.

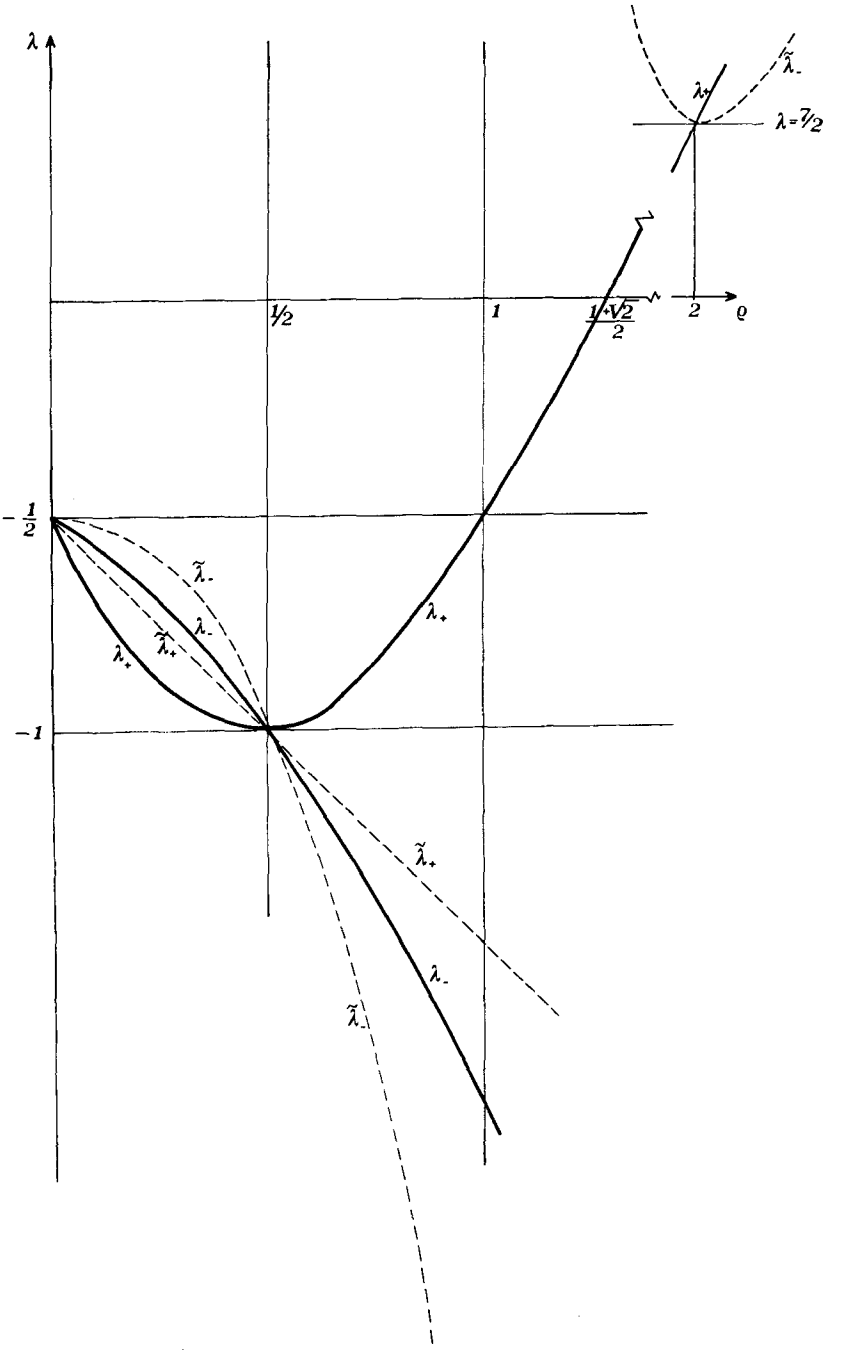

Fig. 4. – The loci of extreme points in the (λ, ϱ)-plane for the surface (14) $\mathscr{L}^2 = \mathscr{L}^2(\lambda, \varrho)$ on the solid curves λ_+ and λ_-; the loci of the points where $\mathscr{L}^2 = \lambda^2$ lie on the dashed curves $\tilde{\lambda}_+$, $\tilde{\lambda}_-$.

Using $\varepsilon = 0$ in eq. (5) and putting $\dot{r} = 0$, we have from (4) and (13) the locus of turning points at

$$\mathscr{L}^2 = \frac{(\lambda + 2\varrho)^2}{(2\varrho - 1)^2} + \varrho^2 + \varrho \,. \tag{14}$$

We shall look for the surface $\mathscr{L}^2 = \mathscr{L}^2(\lambda, \varrho)$. The first ϱ-derivative of (14) is zero along the curves

$$\lambda_+ = 2\varrho^2 - 2\varrho - \tfrac{1}{2} \,, \tag{15}$$

$$\lambda_- = -2\varrho^2 - \tfrac{1}{2} \,. \tag{16}$$

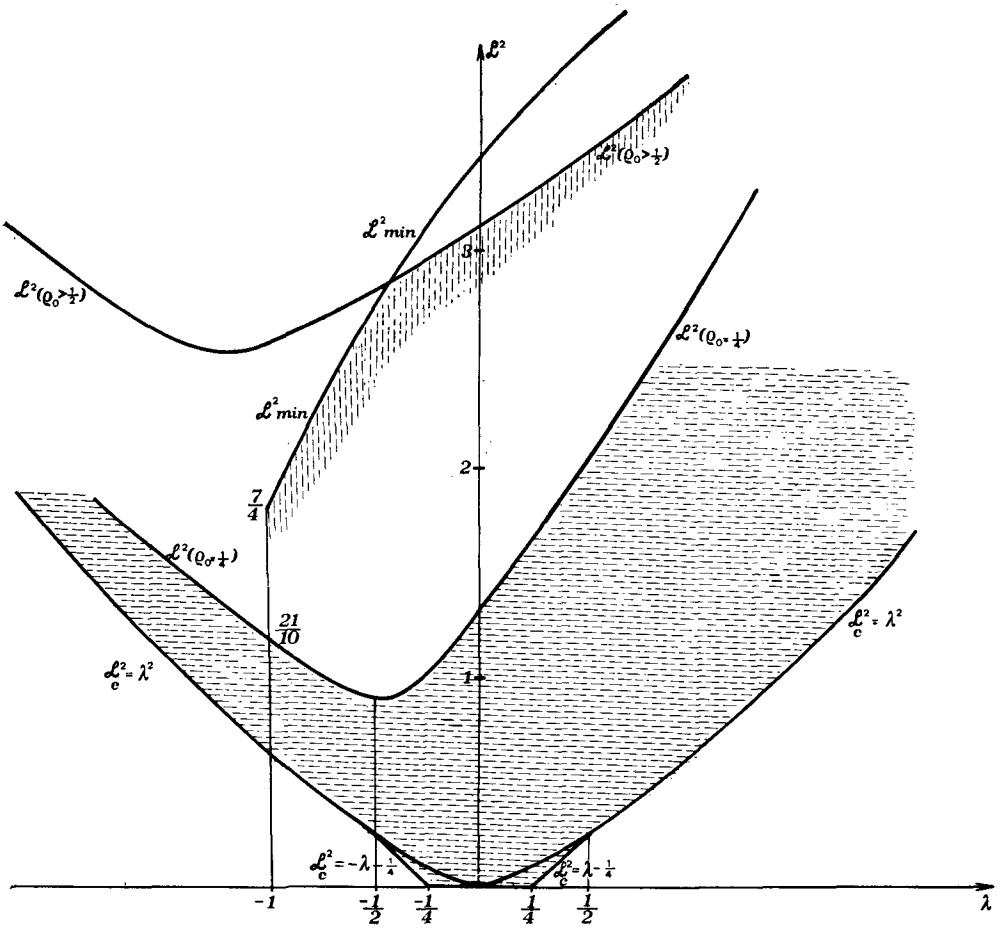

Fig. 5. – The domain for $\mathscr{L}^2$ and λ of permitted emission. It is bounded from below by the composite curve $\mathscr{L}^2_c = \lambda^2$, $|\lambda| > \frac{1}{2}$, $\mathscr{L}^2_c = \pm\lambda - \frac{1}{4}$, $0 < |\lambda| < \frac{1}{2}$, and above from the curver $\mathscr{L}^2(\varrho)$ when $\mathscr{L}^2(\varrho) < \mathscr{L}^2_{\min}$, and $\mathscr{L}^2_{\min}$ otherwise. In the picture are drawn, as an example, the curves $\mathscr{L}^2_{(\varrho=\frac{1}{2})}$ (to scale) and $\mathscr{L}^2_{(\varrho>\frac{1}{2})}$ (not to scale). The other curves are to scale.

The shapes of λ_+ and λ_- are given by the solid lines in Fig. 4. They intersect at $\lambda = -1$; λ_- is the locus of the minimum for $\mathscr{L}^2$, λ_+ is that of the maximum at $\varrho < \frac{1}{2}$, and the minimum again at $\varrho > \frac{1}{2}$.

At $\varrho = \frac{1}{2}$, $\mathscr{L}^2$ diverges positively except for $\Gamma = -1$. From the considerations made in the previous Section, the general motion cannot occur for arbitrary values of $\mathscr{L}$ and λ. In fact we know that for $\mathscr{L}^2 > \frac{1}{4}$ the motion is allowed only with $\mathscr{L}^2 \geqslant \lambda^2$. When $\mathscr{L}^2 \leqslant \frac{1}{4}$, the vortex effect arises for values of λ in the range

$$-\tfrac{1}{2} \leqslant \lambda \leqslant \tfrac{1}{2} . \tag{17}$$

The admissible values of $\mathscr{L}$ and λ for the motion are defined by the shaded regions in Fig. 5. The composite curve which limits form below the allowed domain of $\mathscr{L}$ and λ in Fig. 5 will be called $\mathscr{L}^2_c$. We shall now examine whether turning points occur within the vortex condition (17). The locus of points where

$$\mathscr{L}^2 \leqslant \lambda^2 \tag{18}$$

lies between the two curves

$$\tilde{\lambda}_+ = -(\varrho + \tfrac{1}{2}) , \tag{19}$$

$$\tilde{\lambda}_- = \frac{1 - \varrho + 2\varrho^2}{2(\varrho - 1)} . \tag{20}$$

Their shapes are given by the dashed lines in Fig. 4. We can draw the surface (15) with the help of Fig. 4 and 5, keeping in mind the following properties:

$$\left\{\begin{array}{l} \lim\limits_{\varrho \to 0} \mathscr{L}^2 = \lambda^2 , \qquad \lim\limits_{\varrho \to \frac{1}{2}} \mathscr{L}^2 = \infty , \\ \lim\limits_{\varrho \to \infty} \mathscr{L}^2 = \infty , \qquad \lim\limits_{\varrho \to 0} \mathscr{L}^2_{,\varrho} = (2\lambda + 1)^2 , \\ \mathscr{L}^2 \geqslant \lambda^2 \left\{\begin{array}{l} \varrho > 1 \Rightarrow \left\{\tilde{\lambda}_+ \leqslant \lambda \leqslant \tilde{\lambda}_-\right\} , \\ \varrho < 1 \Rightarrow \left\{\begin{array}{l} \lambda \geqslant \tilde{\lambda}_+ \\ \lambda \leqslant \tilde{\lambda}_- \end{array}\right\} , \end{array}\right. \\ \mathscr{L}^2 \leqslant \lambda^2 \left\{\begin{array}{l} \varrho > 1 \Rightarrow \left\{\begin{array}{l} \lambda \geqslant \tilde{\lambda}_- \\ \lambda \leqslant \tilde{\lambda}_+ \end{array}\right\} , \\ \varrho < 1 \Rightarrow \left\{\tilde{\lambda}_- \leqslant \lambda \leqslant \tilde{\lambda}_+\right\} . \end{array}\right. \end{array}\right. \tag{21}$$

Sections of the surface (15) are then given in Fig. 6 *a*)-*f*). From them we easily recognize that particles moving in vortex with λ as in (17) do not find turning points.

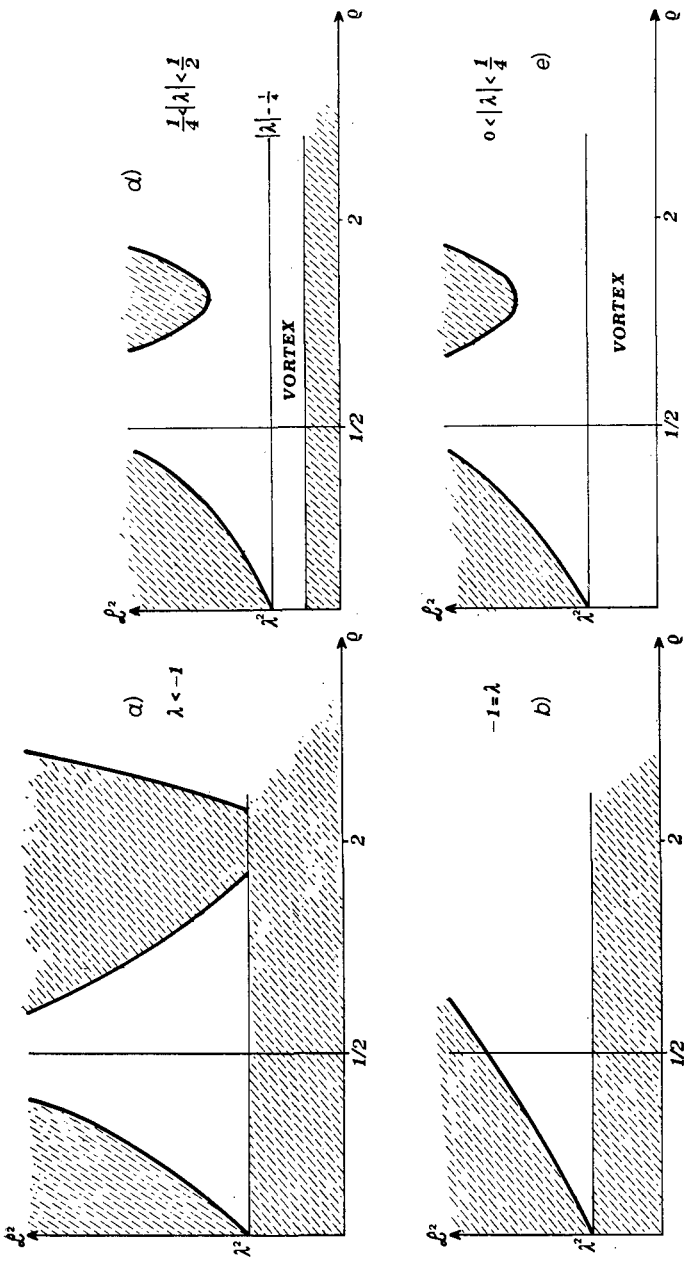

Fig. 6. – Sections of the surface $\mathscr{L}^2 = \mathscr{L}^2(\lambda, \varrho)$ of turning points for photons with $\lambda = \text{const}$. The shaded regions are forbidden to photons. *a*) $\lambda < -1$, *b*) $\lambda = -1$, *c*) $-1 < \lambda \leqslant -\frac{1}{2}$, *d*) $\frac{1}{4} < |\lambda| < \frac{1}{2}$, *e*) $0 < |\lambda| < \frac{1}{4}$, *f*) $\lambda > \frac{7}{2}$.

4. – Conclusion.

The information we have from Fig. 5-6 may be summarized as follows: Ingoing photons with $\lambda < -1$ and $\lambda > \frac{7}{2}$ can never strike the pseudosingularity $\varrho = \frac{1}{2}$. Photons with $\lambda \leqslant -\frac{1}{2}$ can never cross the ring singularity at $\varrho = 0$. Photons with $-\frac{1}{2} \leqslant \lambda \leqslant \frac{1}{2}$ can cross the ring singularity only with $\mathscr{L}^2 < \lambda^2$ and in that case the motion is of spiral type and confined up or down the equatorial plane. For the outgoing photons we can distinguish three cases:

a) Photons emitted at $\underset{0}{\varrho} \geqslant 2$. All radiation can escape to infinity and the allowed values of λ lie in the interval (Fig. 4)

$$\tilde{\lambda}_+(\underset{0}{\varrho}) \leqslant \lambda \leqslant \tilde{\lambda}_-(\underset{0}{\varrho}) , \tag{22}$$

and the corresponding values of $\mathscr{L}^2$ are in the range

$$\mathscr{L}^2_c \leqslant \mathscr{L}^2 \leqslant \mathscr{L}^2(\underset{0}{\varrho}) . \tag{23}$$

The area defined by the limits (22) and (23) (Fig. 4) is proportional to the amount of the emitted radiation.

b) Photons emitted at $\frac{1}{2} < \underset{0}{\varrho} < 2$. Not all the radiation emitted can escape to infinity; the range permitted for λ is now

$$\tilde{\lambda}_+(\underset{0}{\varrho}) \leqslant \lambda \leqslant \tfrac{7}{2} , \tag{24}$$

and the corresponding interval of $\mathscr{L}^2$ for the emission is again (23). In this case however, as we can see from Fig. 4-6, the upper limit for $\mathscr{L}^2$ is given by $\mathscr{L}^2(\underset{0}{\varrho})$ when the minimum of $\mathscr{L}^2(\varrho)$ falls to the left of $\underset{0}{\varrho}$, and is given by $\mathscr{L}^2_{\min}$ otherwise. $\mathscr{L}^2_{\min}$ is the projection on the plane $(\mathscr{L}^2, \lambda)$ of the minimum values of $\mathscr{L}^2$ given by the curve λ_+ in eq. (15). From (15) and (14), we have

$$\mathscr{L}^2_{\min} = \frac{7}{4} + (\lambda + 1) + 2\sqrt{2(\lambda + 1)} . \tag{25}$$

Its shape is given in Fig. 5.

c) Photons emitted at $0 \leqslant \underset{0}{\varrho} < \frac{1}{2}$. No radiation whatsoever can escape to infinity owing to the pseudosingular character of the surface $\varrho = \frac{1}{2}$. The radiation which is trapped inside for the black-hole effect may be released if a slide change in the angular momentum brings $a \geqslant m$. The photons emitted

in this case are characterized by the following parameters:

$$\tilde{\lambda}_{-}(\underset{0}{\varrho}) \leqslant \lambda \leqslant \tfrac{7}{2} \tag{26}$$

and

$$\mathscr{L}_0^2 \leqslant \mathscr{L}^2 \leqslant \begin{cases} \mathscr{L}^2_{\min} \ (\mathscr{L}^2_{\min} < \mathscr{L}^2(\underset{0}{\varrho})) \,, \\ \mathscr{L}^2(\underset{0}{\varrho}) (\mathscr{L}^2_{\min} > \mathscr{L}^2(\underset{0}{\varrho})) \end{cases} \tag{27}$$

(upper curve in Fig. 5).

We notice however that as $\underset{0}{\varrho}$ goes to zero the curve $\mathscr{L}^2(\underset{0}{\varrho})$ becomes $\mathscr{L}^2(\underset{0}{\varrho}) = \lambda^2$, and in that case the dominant emission is confined to the equatorial plane ($\mathscr{L}^2 = \lambda^2$) and to the vortex region (12).

* * *

Thanks are due to Dr. OCCHIONERO for discussions. The financial support of C.N.R. (Comitato Nazionale Ricerche) of Italy is gratefully acknowledged.

● RIASSUNTO

Si analizza il moto geodetico nella metrica di Kerr in condizioni generali con l'ausilio degli integrali primi. Si trova che alcune delle particelle di alta energia e fotoni, trascinati dal campo gravitazionale, si muovono secondo grandi vortici intorno all'asse di rotazione al di sopra ed al di sotto del piano equatoriale.

Орбитальное и вихревое движение в метрике Керра.

Резюме (*). — В общем случае анализируется движение в метрике Керра с использованием первых интегралов. Получается, что некоторые частицы высокой энергии и фотоны движутся в гигантском завихрении вокруг оси симметрии выше и ниже экваториальной плоскости, увлеченные гравитационным полем.

(*) *Переведено редакцией.*